Structural Variation in the Antithrombin III Binding Site Region and Its Occurrence in Heparin from Different Sources†

Duraikkannu Loganathan,‡ Hui M. Wang,‡ Larry M. Mallis,§ and Robert J. Linhardt*,‡

Division of Medicinal and Natural Products Chemistry, College of Pharmacy, and High Resolution Mass Spectrometry Facility, University of Iowa, Iowa City, Iowa 52242

Received September 27, 1989; Revised Manuscript Received December 7, 1989

ABSTRACT: A tetrasaccharide possessing a biosynthetically permissible structural variability in and adjacent to the antithrombin III (ATIII) binding site has been isolated from heparin lyase depolymerized bovine lung heparin by using strong anion-exchange high-pressure liquid chromatography (SAX-HPLC). On the basis of two-dimensional 500-MHz ^{1}H NMR experiments, including phase-sensitive correlated spectroscopy (COSY) and rotating frame nuclear Overhauser enhancement spectroscopy (ROESY), and fast-atom bombardment mass spectrometry (FAB-MS), the primary structure of this tetrasaccharide was unambiguously established as ΔUAp2S (1→4)-α-D-GlcNp2S6S(1→4)-β-D-GlcAp(1→4)-α-D-GlcNp2S3S6S (where ΔUA represents 4-deoxy-α-L-*threo*-hex-4-enopyranosyluronic acid). The ^{1}H NMR ROESY experiment proved to be particularly valuable in offering sequence information. Heparins from a variety of species and tissue sources were examined by oligosaccharide mapping using SAX-HPLC and gradient polyacrylamide gel electrophoresis. Two of these heparins are used as anticoagulants; they are porcine intestinal mucosal heparin and bovine lung heparin. The predominant ATIII-binding site in porcine heparin contained an N-acetylated glucosamine residue. We now report the structure of the predominant ATIII-binding site in bovine heparin as →4)-α-D-GlcNp2S6S(1→4)-β-D-GlcAp(1→4)-α-D-GlcNp2S3S6S(1→4)-α-L-IdoAp2S(1→4)-α-D-GlcNp2S6S(1→. This study shows the presence of one or both types of ATIII-binding-site variants in all of the heparins that were examined.

Heparin is a polydisperse sulfated copolymer of 1→4-linked glucosamine and uronic acid residues and has been used clinically for over 50 years as an anticoagulant (Casu, 1985). Although the major trisulfated disaccharide repeating unit of heparin is →4)-2-deoxy-2-sulfamido-α-D-glucopyranose 6-sulfate-(1→4)-α-L-idopyranosyluronic acid 2-sulfate-(1→, substantial sequence variability is observed in this polysaccharide (Bienkowski & Conrad, 1985; Merchant et al., 1985).

Heparin biosynthesis begins with the assembly of a core protein and the O-glycosylation of serine residues to form a trisaccharide linkage region. This linkage region grows by alternate addition of 2-deoxy-2-acetamido-D-glucopyranose and D-glucopyranosyluronic acid leading to a linear 1→4-linked polysaccharide. The sequential action of enzymes that partially N-deacetylate, N-sulfate, C5-epimerize, and O-sulfate the homocopolymer chain gives heparin its complex structure and its microheterogeneity (Comper, 1981; Lindahl & Kjellen, 1987; Lindahl et al., 1986). In the final step of heparin biosynthesis specific glucosamine residues in the polysaccharide chain are 3-O-sulfated (Lindahl et al., 1986). This step is particularly noteworthy as it generally results in sites at which the serine protease inhibitor antithrombin III (ATIII)[1] can tightly bind. A specific pentasaccharide sequence in porcine heparin, representing the minimal binding site for ATIII (Figure 1), has been shown to be largely responsible for heparin's anticoagulant activity (Lindahl et al., 1983; Atha et al., 1984). Recently, analysis of various heparins led to the proposal of structural variability of heparin's ATIII-binding site (Lindahl et al., 1984; Pejler et al., 1987; Guo & Conrad, 1989). The precise structure of the ATIII-binding site within bovine heparin has not been reported, despite the fact that bovine heparin is used as frequently as porcine heparin in clinical anticoagulation.

As part of our continuing structural studies on heparin we reported the structural characterization by NMR and mass spectrometry of a hexasaccharide (**7**) (Figure 1). This hexasaccharide contained a portion of an ATIII-binding site that was purified from porcine mucosal heparin following its depolymerization using flavobacterial heparinase (Linhardt et al., 1986). Herein, we report the isolation and characterization, using advanced NMR methods including two-dimensional COSY and ROESY (Bax & Davies, 1985), of a tetrasaccharide (**6**) obtained from bovine lung heparin. The distribution of this new structural variant of the ATIII-binding site in heparin obtained from a variety of species and tissue sources is also described.

Experimental Procedures

Materials

All the heparins used in this study were in the sodium salt form. Porcine mucosal heparin (164 USP units/mg) was from Hepar Industries, Franklin, OH, and ovine intestinal heparin (182 units/mg) was from Sigma Chemical Co., St. Louis, MO.

† This work was supported by National Institutes of Health Grants HL29797 and GM38060.

* To whom correspondence should be addressed.

‡ Division of Medicinal and Natural Products Chemistry.

§ High Resolution Mass Spectrometry Facility.

[1] Abbreviations: ATIII, antithrombin III; ΔAU, 4-deoxy-α-L-*threo*-hex-4-enopyranosyluronic acid; GlcNp2S, 2-deoxy-2-sulfamidoglucopyranose; GlcNAcp, 2-deoxy-2-acetamidoglucopyranose; IdoAp, idopyranosyluronic acid; GlcNAp, glucopyranosyluronic acid; S, sulfate; SAX-HPLC, strong anion-exchange high-pressure liquid chromatography; PAGE, polyacrylamide gel electrophoresis; 2D NMR, two-dimensional nuclear magnetic resonance; COSY, correlated spectroscopy; ROESY, rotating frame nuclear Overhauser enhancement spectroscopy; FAB-MS, fast atom bombardment mass spectrometry.

0006-2960/90/0429-4362$02.50/0

Bovine lung heparin (131 units/mg), bovine intestinal heparin (152 units/mg), bovine pancreatic heparin (67 units/mg), bovine placental heparin (143 units/mg), hen intestinal heparin (149 units/mg), and clam heparin (168 anti Xa units/mg) were generously provided by Professor Bianchini, Opocrin, Corlo, Italy. Heparinase, heparin lyase (EC 4.2.2.7) having a specific activity of 5 IU/mg, was prepared and purified as previously reported (Galliher et al., 1981; Yang et al., 1985) or was obtained from Sigma. Spectropore dialysis tubing (M_r cutoff = 1000) was purchased from Spectrum Medical, Los Angeles, CA. Polyacrylamide P2 gel for desalting was from Bio-Rad, Richmond, CA. HPLC was performed by using dual LDC Constametric III pumps with gradient mixer and microprocessor gradient control and data collection using a Rheodyne injector on a Phase Separations, Norwalk, CT, SAX column (4.6 × 250 mm analytical column and a 20 × 250 mm semipreparative column, both of 5-μm particle size) and an ISCO Model 1840 variable-wavelength UV detector. Gradient polyacrylamide gel electrophoresis was performed on a Hoeffer SE620 (San Francisco, CA) slab gel cell using a Bio-Rad 1420B power supply. High-purity electrophoresis reagents were purchased from IBI, Inc., New Haven, CT. Spectrometric measurements were performed on a Shimadzu UV-160 spectrophotometer, Bruker AM500 MHz (at the National Magnetic Resonance Facility at Madison, WI) NMR spectrometer with an ASPECT 3000 computer, and a VG ZAB-HF mass spectrometer. ^2H_2O (99.996 atom %) and TSP-d_4 (NMR chemical shift standard) were from Aldrich Chemical Co., Milwaukee, WI.

Methods

Preparation of Heparin Samples. Approximately 20 mg of each heparin was dissolved in 10 mL of distilled water and dialyzed exhaustively, freeze-dried, and prepared at exactly 20.0 mg/mL in distilled water (Linhardt et al., 1988).

Heparinase Depolymerization of Heparin. To 50 μL of each heparin sample (20 mg/mL) was added 450 μL of sodium phosphate buffer (5 mM sodium phosphate, pH 7, and 200 mM sodium chloride) containing 15 mIU heparinase. The reaction mixture was incubated at 30 °C for 8 h. At reaction completion the depolymerization mixture was frozen and stored at −70 °C.

HPLC Analysis of Depolymerized Heparins. Depolymerized heparin was analyzed at two concentrations (40 μg/40 μL and 4 μg/40 μL) on an analytical SAX-HPLC column. The sample was eluted from the column by using a 150-mL linear gradient (0.2–1.0 M) of sodium chloride at pH 3.5 at a flow rate of 1.5 mL/min. The elution profile was monitored by absorbance at 232 nm at 0.02 absorbance unit full scale (AUFS) and a chart speed of 15 cm/h. Retention time varies due to aging of the columns (Rice et al., 1985) so that peaks were tentatively identified by coelution with an authentic sample. The amount of each component was measured by integration of peak area using a standard curve.

Gradient PAGE Analysis of Depolymerized Heparins. Depolymerized heparin was analyzed by applying sample (20–40 μg in 50 μL) to a discontinuous PAGE gel (Rice et al., 1987) using a linear acrylamide and cross-linked gradient (12–22% total acrylamide). Two gels (16 × 32 × 0.15 cm) were run simultaneously at 400 V for 17 h, by which time the added bromophenol blue marker dye had migrated 18 cm into the resolving gel. The gels were removed from the glass plates and stained for 30 min in Alcian Blue 0.5% (w/v) in 2% (v/v) aqueous acetic acid destained with successive washes of 2% acetic acid. Bands were identified by comigration with authentic samples.

Preparative HPLC of Oligosaccharides. Oligosaccharides **1–5** and **7** (35 mg) were prepared from (900 mg) heparinase (5 IU/mg, purified in our laboratory) depolymerized porcine mucosal heparin by using semipreparative SAX-HPLC as previously described (Rice & Linhardt, 1989). The structures of oligosaccharides **1–5** are as follows: **1**, ΔUAp2S(1→4)-α-D-GlcNp2S; **2**, ΔUAp2S(1→4)-α-D-GlcNp2S6S; **3**, ΔUAp2S(1→4)-α-D-GlcNp2S(1→4)-α-L-IdoAp2S(1→4)-α-D-GlcNp2S6S; **4**, ΔUAp2S(1→4)-α-D-GlcNp2S6S(1→4)-β-D-GlcAp(1→4)-α-D-GlcNp2S6S; and **5**, ΔUAp2S(1→4)-α-D-GlcNp2S6S(1→4)-α-L-IdoAp2S(1→4)-α-D-GlcNp2S6S. Analysis on analytical SAX-HPLC and gradient PAGE demonstrated the sample purity to be >95%.

Oligosaccharide **6** was prepared by heparinase (0.5 IU of 5 IU/mg enzyme, purified in our laboratory) depolymerization of bovine lung heparin (1 g). The oligosaccharide mixture (1 g in 10 mL) was loaded in five separate injections to the semipreparative column. The peak eluting at 0.75–0.78 M sodium chloride was collected. The five runs were pooled, freeze-dried, desalted on a 2.5 × 35 cm P2 column at 1 mL/min, and again freeze-dried. The crude oligosaccharide **6** (20 mg, 70% pure by analytical SAX-HPLC) was again applied to semipreparative SAX-HPLC in a single injection (20 mg in 1 mL) and collected, desalted, and freeze-dried as before. The resulting oligosaccharide **6** (10 mg) was >95% pure by analysis using SAX-HPLC and gradient PAGE.

Spectrometric Methods. Ultraviolet absorbance was determined at 232 nm by weighing salt-free sample and dissolving in 0.03 N hydrochloric acid. NMR was performed on a Bruker AM500 spectrometer (^1H at 500 MHz). Samples were prepared for ^1H NMR (400 μL at 9.4 mM) in pH 7.08, 50 mM sodium phosphate buffer in D_2O, after exchange in D_2O. The spectra were obtained at 298 K. Two-dimensional ^1H COSY and ^1H ROESY NMR spectra each required 10 of acquisition time and used Bruker software. Mass spectrometric analysis was performed by using a VG ZAB-HF mass spectrometer, equipped with an ION TECH 11 NF saddle field atom gun (xenon at 8 kV, 1.5 mA), in the fast atom bombardment (FAB) ionization mode. Negative ion FAB spectra were obtained in both low- and high-resolution (for accurate measurements) modes by signal adding eight scans using the multichannel analysis scanning software of the 11-250 J data system. Samples were prepared for FAB analysis by dissolving 200 μg of oligosaccharide in approximately 10 μL of distilled water. Typically, 1 μL of triethanolamine is placed on the FAB probe tip (as matrix) to which 1 μL of the oligosaccharide solution is added (Mallis et al., 1989).

Coagulation and Amidolytic Assays. Oligosaccharide samples were assayed for both anti-factor IIa and anti-factor Xa activities by the "end point" method using amidolytic substrates against a standard curve constructed by using USP heparin (Linhardt et al., 1988).

Results and Discussion

Heparin lyase acts on heparin linkages having the structures →4)-α-D-GlcNp2S6S(1→4)-α-L-IdoAp2S(1→, →4)-α-D-GlcNp2S(1→4)-α-L-IdoAp2S(1→, and →4)-α-D-GlcNp2S3S6S(1→4)-α-L-IdoAp2S(1→ (Rice & Linhardt, 1989). Oligosaccharide mapping has been used to study porcine mucosal heparins from a variety of commercial sources. These were depolymerized by using heparin lyase, and a small number of major oligosaccharide products were obtained. When contaminating dermatan/chondroitin sulfates (0.6–7.4 wt %) were taken into account, 91 wt % of heparin's mass could be ascribed to oligosaccharides of known structure (Linhardt et al., 1988). Porcine mucosal heparin and bovine

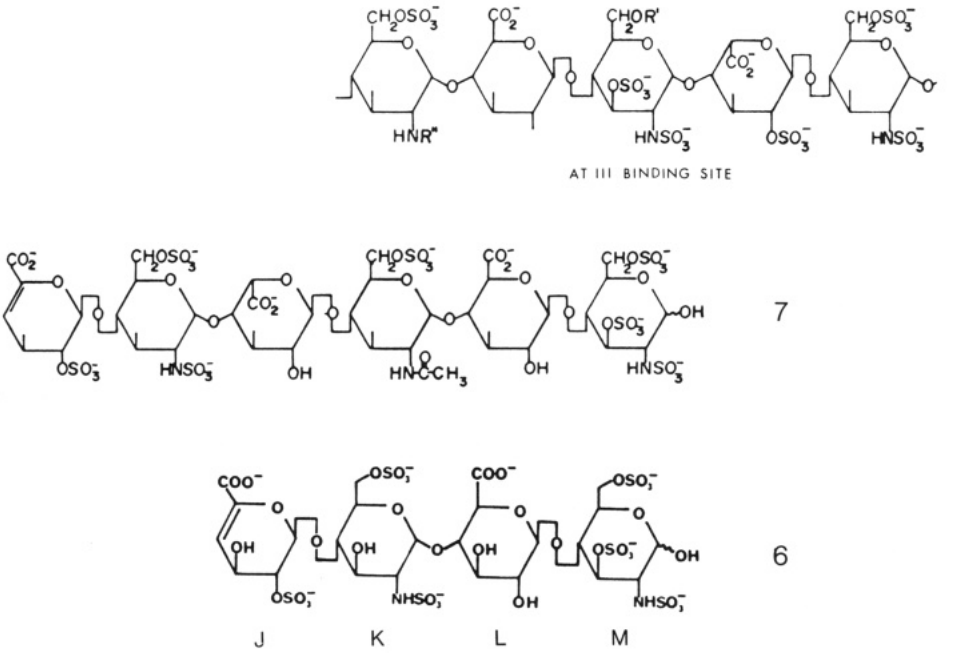

FIGURE 1: Structures of heparin's ATIII-binding site (R = H or SO_3^-) including the permissible structural variation where R″ = SO_3^- or $COCH_3$ (Pejler et al., 1987), hexasaccharide **7** (Linhardt et al., 1986), and tetrasaccharide **6**.

lung heparin showed distinctly different oligosaccharide maps.

The structure of hexasaccharide **7**, recovered from heparin lyase depolymerized porcine mucosal heparin (Figure 1), contains a portion of heparin's ATIII-binding site and was previously reported (Linhardt et al., 1986) to be ΔUAp2S-(1→4)-α-D-GlcNp2S6S(1→4)-α-L-IdoAp(1→4)-α-D-GlcNAcp6S(1→4)-β-D-GlcAp(1→4)-α-D-GlcNp2S3S6S. The amount of hexasaccharide **7** observed in oligosaccharide maps of bovine lung heparin (having comparable ATIII-mediated activities to porcine mucosal heparin) was greatly reduced, while a second unidentified oligosaccharide **6** eluting prior to oligosaccharide **7** on SAX-HPLC was observed. The coenrichment of oligosaccharides **6** and **7**, in porcine mucosal heparin which had been ATIII-affinity fractionated, suggested that oligosaccharide **6** might correspond to a portion of one of the proposed structural variants of heparin's ATIII-binding site (Pejler et al., 1987). Recently, we demonstrated that the concentration of oligosaccharide **6** found in oligosaccharide maps of fractionated bovine heparins (and that of hexasaccharide **7** in porcine heparins) correlated with the ATIII-mediated anti-IIa activity of these fractionated heparins (Kim & Linhardt, 1989).

Bovine lung heparin (1 g) was depolymerized by using heparin lyase, and following repeated SAX-HPLC purification, oligosaccharide **6** (10 mg) was recovered (2.01 wt % of **6** was present in bovine lung heparin as determined by analytical SAX-HPLC). This oligosaccharide was judged to be >95% pure by chromatographic analysis and electrophoresis. The ultraviolet spectrum comparable to those determined for oligosaccharides **1**–**5** and **7** (Linhardt et al., 1988), indicated the presence of a ΔUAp2S residue at the nonreducing end of oligosaccharide **6**. High-resolution negative-ion FAB-MS analysis gave an intense molecular ion at m/z 1306.8112 (Δm = −2.8 mmu) assigned to $[\mathbf{6} + 7Na^+]^-$ (Mallis et al., 1989), consistent with oligosaccharide **6** having a molecular formula of $C_{24}H_{30}N_2S_6O_{38}N_8$. Within the framework of heparin's known structural features, this molecular formula supports the assignment of oligosaccharide **6** structure as a hexasulfated tetrasaccharide having an unsaturated nonreducing terminus and containing no *N*-acetyl residue. Low-resolution FAB-MS established the sulfation of each sugar residue in tetrasaccharide **6** from fragmentation pattern (Figure 2). In the molecular ion region of the spectrum, ions corresponding to attachment of six to eight sodium ions (Na^+) are observed at m/z 1285, 1307, and 1329, respectively. Assuming the oligosaccharide to be fully sodiated, these ions correspond to $[M - 2Na^+ + H^+]^-$, $[M - Na^+]^-$, and $[M - H^+]^-$, respectively. It is interesting to note that although the oligosaccharide is thoroughly desalted, ions corresponding to NaCl addition to the molecular ion are observed. These ions, at m/z 1365 and 1423, correspond to addition of one and two molecules of NaCl to the molecular ion at m/z 1307. It is the complexing of these highly sulfated oligosaccharides to NaCl that makes FAB mass spectrometry so difficult. The predominant fragment ions observed correspond to loss of $NaSO_3^-$ with proton addition at m/z 1205 and 1103 (Mallis et al., 1989). Structurally significant fragment ions are observed at m/z 1025 and 642 and are assigned to loss of the reducing end sugar and loss of the two nonreducing end sugars, respectively.

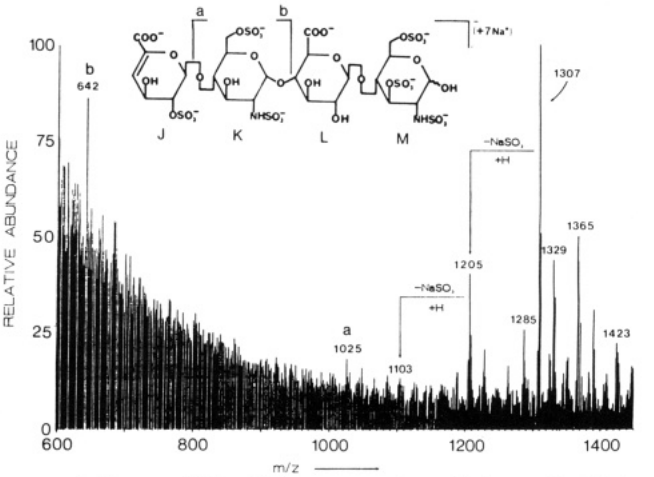

FIGURE 2: Low-resolution FAB mass spectrum of oligosaccharide **6** (≈20 μg) recorded in the negative ion mode using triethanolamine as the matrix.

High-field NMR spectroscopy proved to be the most useful tool in unambiguously assigning the structure of tetrasaccharide **6**. Starting from the nonreducing end, the sugar

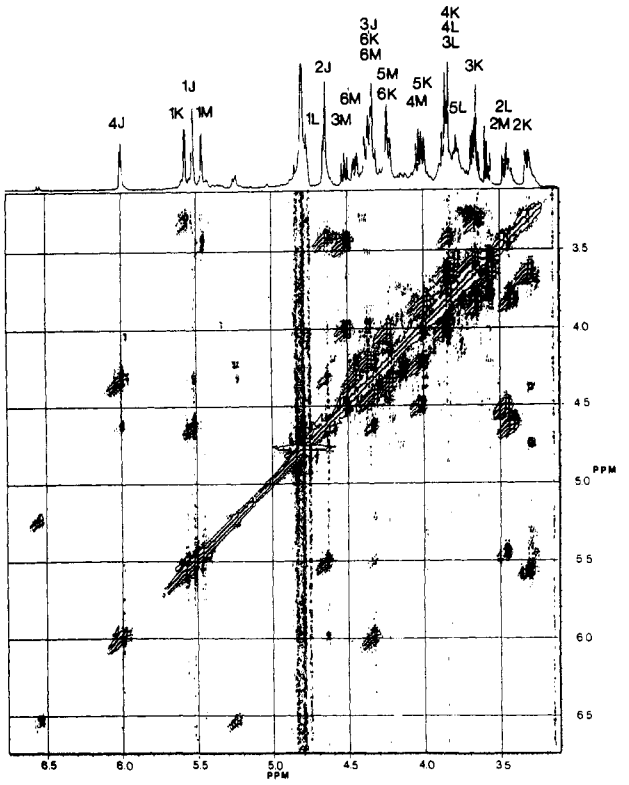

FIGURE 3: 500-MHz ^{1}H NMR phase-sensitive COSY spectrum of **6** (D_2O, 298 K). Spectral parameters are 2048 data points in the F_2 dimension, 512 data points in the F_1 dimension, and zero-filling performed in the F_1 dimension to 1012 data points. Assignments of all proton signals are indicated in the one-dimensional spectrum at the top of the figure.

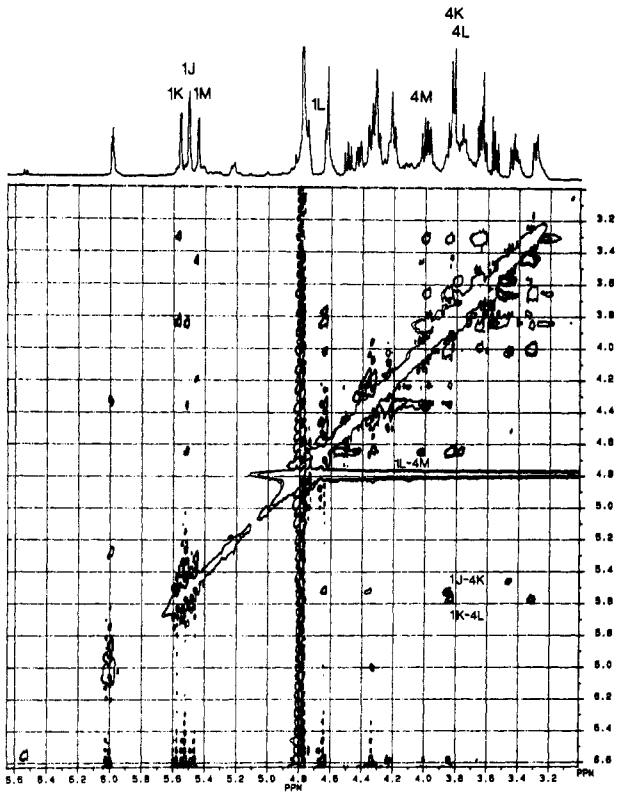

FIGURE 4: 500-MHz ^{1}H NMR ROESY spectrum of **6** (D_2O, 298 K). Spectral parameters are the same as in Figure 3, and a mixing time of 180 ms was used. Assignments of only the important NOE cross-peaks are shown.

residues in **6** are designated as J, K, L, and M (see Figure 1). The 500-MHz ^{1}H NMR spectrum of **6** (not shown) recorded in D_2O gave four, well-resolved, single-proton resonances in the 4.9–6.0 ppm region. Comparison of the chemical shift and coupling constant values of these resonances with those of already reported heparin-derived tetrasaccharides (Merchant et al., 1985; Linker & Hovingh, 1984) and hexasaccharide **7** containing a portion of ATIII-binding site (Linhardt et al., 1986; Petitou et al., 1988) quickly narrowed down the structural possibilities of **6**. The presence of only three anomeric proton resonances at 5.56, 5.51, and 5.45 ppm (the signal at 6.00 ppm being assigned to JH-4) indicates the upfield shift of the fourth anomeric proton. Knowing the reported chemical shift (≈5.2 ppm) of L-idopyranosyluronic acid 2-*O*-sulfate anomeric proton and that of unsulfated L-idopyranosyluronic acid residue (≈5.0 ppm), the absence of major resonances in the 4.90–5.30 ppm region for **6** indicated that internal uronic acid was D-glucuronic acid.

The 500-MHz ^{1}H NMR two-dimensional phase-sensitive COSY spectrum (Figure 3) provided complete spin connectivity information. Starting with the signal at 6.00 ppm (JH-4), a pair of cross-peaks establish its connectivity to the JH-3 resonance at 4.32 ppm, which in turn shows connectivity to the JH-2 resonance at 4.63 ppm. Further connectivity to the JH-1 resonance at 5.51 ppm completes the identification of all resonances of residue J. Likewise, starting from the anomeric proton resonance at 5.45 ppm, all the resonances of residue M are easily identified. Excellent agreement between the chemical shift and coupling constant data of all protons of J and M residues in **6** with those reported for the nonreducing and reducing end residues, respectively, in **7** (Linhardt et al., 1986; Petitou et al., 1988) clearly confirms the 3-O-sulfation (4.50 ppm MH-3) in residue M and 2-O-sulfation in residue J of **6** (4.63 ppm JH-2). The third anomeric proton resonance at 5.56 ppm assignable to the internal glucosamine moiety shows connectivity to the KH-2 resonance at 3.30 ppm. Moving further in the downfield, the rest of the residue K resonances are easily identified. These data are in accordance with a 2-deoxy-2-sulfamido-α-D-glucopyranose 6-*O*-sulfate structure for residue K. Finally, the resonance at 4.64 ppm (seen overlapping with that of JH-2) assignable to the anomeric proton of D-glucuronic acid shows cross-peaks with the H-2 resonance at 3.42 ppm. This value is very close to that reported for H-2 of the corresponding residue in **7** (Linhardt et al., 1986; Petitou et al., 1988), indicating the absence of 2-*O*-sulfate. The rest of the resonances of residue L in **6** are easily identified. Thus, the ^{1}H NMR spectrum of **6** was completely assigned. The small signal appearing at 5.25 ppm might be assignable to the anomeric proton of a minor impurity that contains an IdoAp2S residue, while those at 6.55, 3.67, and 3.58 ppm could not be assigned.

To confirm the above spectral assignments and to establish the sequence in **6**, a two-dimensional rotating frame nuclear Overhauser enhancement spectrum (ROESY, Figure 4) was recorded. The choice of ROESY for **6** was governed by the fact that the two-dimensional NOESY experiment gives rise to unobservably small NOEs for medium-sized oligosaccharides when $\omega_0 t_c$, the product of spectrometer frequency and molecular rotational correlation time, is approximately equal to unity (as it happens at 500 or 600 MHz for medium-sized molecules).

Although a change in temperature or lowering of field strength would enhance the NOE effects in NOESY, the latter option is not preferred due to loss in resolution. A 500-MHz phase-sensitive NOESY run at 10 °C was reported (Ragazzi et al., 1987) to give both intra- and interresidue negative NOE effects for the ATIII-binding pentasaccharide. Very recently the use of ROESY for the conformational analysis of milk

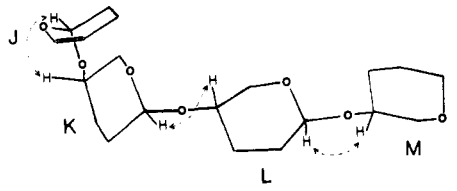

FIGURE 5: Conformation of sugar rings J–M in tetrasaccharide **6**. Dotted lines show the relationships JH1–KH4, KH1–LH4, and LH1–MH4 which display intense cross-peaks in the 500-MHz ^{1}H ROESY spectrum (Figure 4).

Table I: 500-MHz ^{1}H NMR Spectral Assignments (D_2O, TSP-d_4) of Oligosaccharide **6** (Shifts in ppm)

ring	H-1	H-2	H-3	H-4	H-5	H-6	H-'6
J	5.51	4.63	4.32	6.00			
K	5.56	3.30	3.68	3.84	4.00	4.22	4.33
L	4.64	3.42	3.83	3.82	3.78		
M	5.45	3.45	4.50	4.01	4.20	4.34	4.44

oligosaccharides was reported (Breg et al., 1988). We preferred to explore the applications of ROESY to the tetrasaccharide **6** since no change in temperature is needed in this case, and therefore the observed NOEs would be useful in determining the secondary structure of such oligosaccharides at ambient/biological temperatures.

The 500-MHz ROESY spectrum of **6** is shown in Figure 4. The very intense cross-peaks for the following sets of protons (Figure 5) unambiguously establish the sequence in **6**: JH1–KH4 (5.51, 3.84); KH1–LH4 (5.56, 3.82); LH1–MH4 (4.64, 4.01 ppm). In addition, intraresidue NOEs are observed for all protons that are in 1,3-diaxial disposition in each residue. Thus, the primary structure of **6** was unambiguously established. Table I summarizes the chemical shfit data for oligosaccharide **6**.

Oligosaccharide **6** was tested for anticoagulant activity by using amidolytic assays and showed slight (0.8 unit/mg) ATIII-mediated factor Xa activity, while its ATIII-mediated anti IIa activity was negligible. These results were expected as **6** represents only a portion of an intact ATIII-binding site (Figure 1).

The structure assigned to tetrasaccharide **6** is similar to that of hexasaccharide **7**, both having identical disaccharides at their reducing ends. The third sugar residue from the reducing end of each is GlcN6S, which is either N-acetylated or N-sulfated in **7** and **6**, respectively. The fourth sugar residue from the reducing terminus (the nonreducing terminus in tetrasaccharide **6**) is IdoAp and ΔUAp2S in **7** and **6**, respectively. The absence of a 2-sulfate group at this position in **7** makes the linkage at the 4-position of this residue stable on treatment with heparin lyase (Rice & Linhardt, 1989). The presence

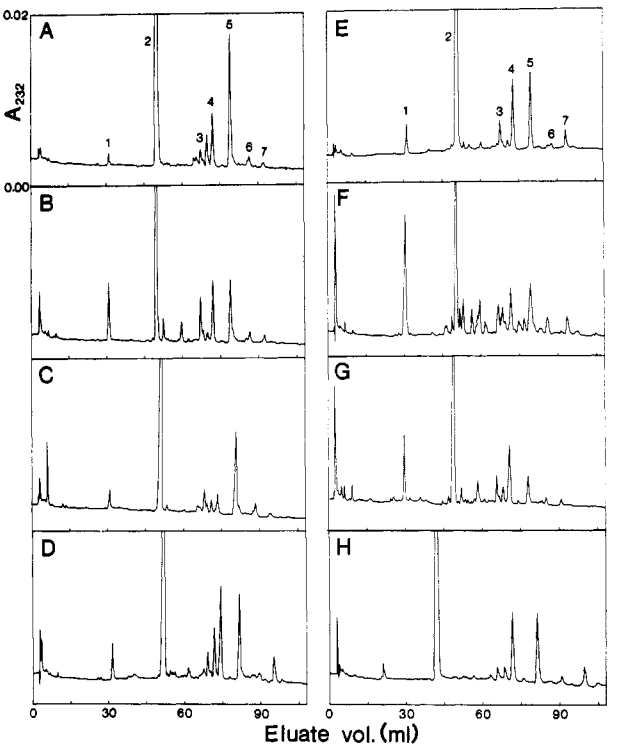

FIGURE 6: SAX-HPLC oligosaccharide maps of heparin A–H from various tissues and species. The retention times observed for heparin H oligosaccharides are different (**1** and **2** eluting early with **6** and **7** eluting late) as this analysis was performed earlier on an older column.

of a 2-*O*-sulfate group at the nonreducing terminus in **6** suggests the ΔUAp2S was originally IdoAp2S and that the next sugar residue was GlcNp2S (sulfation at either the 3- and/or 6-position is also possible), representing a heparin lyase (Rice & Linhardt, 1989) cleavable site. The results described above indicate that the primary ATIII-binding site in porcine mucosal heparin contains a →4)-α-L-IdoAp(1→4)-α-D-GlcNAcp6S sequence at its nonreducing end border, while the primary ATIII-binding site in bovine lung heparin contains a →4)-α-L-IdoAp2S(1→4)-α-D-GlcNp2S6S sequence at its nonreducing end border.

Additional heparins (A–E) were examined by oligosaccharide mapping on SAX-HPLC (Figure 6) and gradient PAGE (Figure 7) in an effort to understand the relationship between the structure of the ATIII-binding site and the type of tissue or the species from which a heparin is prepared. The results obtained with SAX-HPLC and gradient PAGE mapping are qualitatively similar. Oligosaccharides **1**–**7** were identified by coinjection or coapplication of oligosaccharide

Table II: Compositional Analysis of Heparins from Various Species and Tissues

			μg of oligosaccharide[a]/100 μg of heparin							
sample	species	tissue	**1**	**2**	**3**	**4**	**5**	**6**	**7**	Σ μg of oligosaccharides
A	bovine	lung	0.58	54.60	2.18	8.24	18.97	2.01	1.92	88.5
B	bovine	intestine	2.78	39.06	5.81	8.95	8.32	2.02	2.29	69.2
C	bovine	pancreas	0.78	24.84	2.38	2.74	8.59	1.72	1.83	41.0
D	bovine	placenta	2.04	29.43	4.20	8.72	14.07	2.33	7.25	68.1
E	porcine	intestine	1.17	41.81	3.19	8.43	8.36	1.05	3.75	67.8
F	clam		5.56	11.65	4.24	6.06	10.46	2.80	3.96	44.7
G	hen	intestine	3.55	25.20	3.33	8.91	5.10	1.47	2.12	49.7
H	ovine	intestine	0.76	42.22	2.42	12.38	11.82	3.08	5.63	78.3

[a] Oligosaccharides were identified by coelution (and comigration on gradient PAGE) with authentic standards. In the case of bovine lung heparin (A) and porcine intestinal heparin (E), oligosaccharides **1**–**6** and **1**–**5** and **7**, respectively, were isolated and characterized spectroscopically. Oligosaccharide **6** from bovine lung heparin and **7** from porcine intestinal heparin could not be isolated in quantities sufficient for spectral characterization. Concentrations were calculated based on analysis of 4- and 40-μg samples as previously described in detail (Linhardt et al., 1988).

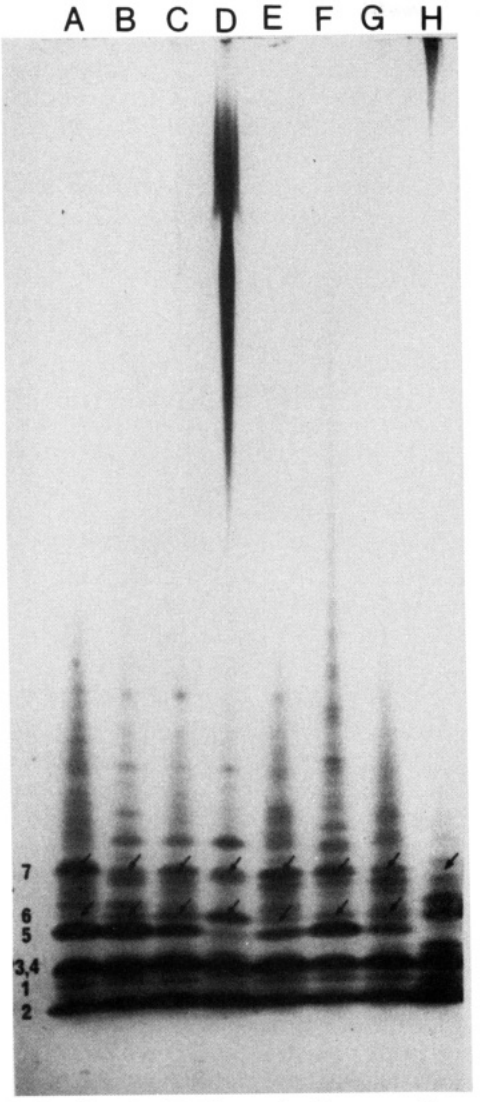

FIGURE 7: Gradient PAGE oligosaccharide maps of heparin from various tissues and species (A–H). Numbers on the left-hand side refer to the oligosaccharide assignments for lanes A–H. Arrows are drawn in each lane that point out the bands corresponding to oligosaccharide standards **6** and **7**.

standards. Quantitative results can be obtained by SAX-HPLC (Linhardt et al., 1988). Standard curves were constructed from pure oligosaccharide standards **1–7** using both 40- (Figure 6) and 4-μg (not shown) injections (Table II). All heparins examined contained peaks or bands coeluting or comigrating with one or both of the ATIII-binding site variants. The species from which a heparin is derived appears to play the dominant role in the major ATIII-binding site structure found. Some variation of ATIII-binding site composition is also seen between heparins from different tissues within a single species. The observation of nondepolymerized polymeric material in several lanes of the gradient PAGE gel (Figure 7) confirms the suspicion that these samples contain dermatan sulfate (Perlin & Folkman, 1987) as a contaminant. The most complex heparin studied was from clam. This observation is consistent with the report (Pejler et al., 1987) of a structural variant from clam heparin which was tentatively identified as →4)-α-D-GlcNp2S-(1→4)-α-L-IdoAp-(1→4)-α-D-GlcNp2S3S6S-(1→. We cannot, however, confirm this structure on the basis of our current study.

In conclusion, we have determined the structure of the major ATIII-binding site in bovine heparin using FAB-MS and two-dimensional ^{1}H NMR spectroscopy. The structure of the ATIII-binding site in bovine heparin is the same as one tentatively proposed as a minor ATIII-binding site in porcine heparin (Lindahl et al., 1984) and contains biosynthetically permissible structural variations in and adjacent to the ATIII-binding site. Examination of heparins from a variety of species and tissue sources confirms the widespread presence of this ATIII-binding site structural variant (bovine heparin containing the greatest amount) along with the previously reported ATIII-binding site. Additional studies will be needed to isolate and characterize the remaining structural variants of the ATIII-binding site which have either been tentatively identified or proposed. It is interesting to speculate as to whether ATIII prepared from different species would bind to these binding-site variants with different affinity. Also, further study is needed to correlate the enzyme levels (*O*-sulfotransferase) in different tissues with the final products of heparin's biosynthesis.

ACKNOWLEDGMENTS

We thank Professor Bianchini of Opocrin for providing many of the heparins that were examined in this study and Dr. Ali Al-Hakim of our laboratory for performing the gel electrophoresis experiment. We acknowledge the National Magnetic Resonance Facility at the University of Wisconsin, Madison, for access to high-field NMR instrumentation and Brian Stockman for his assistance.

REFERENCES

Atha, D. H., Stephens, A. W., & Rosenberg, R. D. (1984) *Proc. Natl. Acad. Sci. U.S.A. 81*, 1030–1034.

Bax, A., & Davies, G. D. (1985) *J. Magn. Reson. 63*, 207–211.

Bienkowski, M. J., & Conrad, H. E. (1985) *J. Biol. Chem. 260*, 356–365.

Breg, J., Romijn, D., Vliegenthart, J. F. G., Strecker, G., & Montreul, J. (1988) *Carbohydr. Res. 183*, 19–34.

Casu, B. (1985) *Adv. Carbohydr. Chem. Biochem. 43*, 51–134.

Comper, W. D. (1981) *Heparins (and related polysaccharides)* (Huglin, M. B., Ed.) Polymer Monographs, Vol. 7, Gordon and Science, New York.

Galliher, P. M., Cooney, C. L., Langer, R., & Linhardt, R. J. (1981) *Appl. Environ. Microbiol. 41*, 360–365.

Guo, Y., & Conrad, H. E. (1989) *Anal. Biochem. 176*, 96–104.

Kim. Y. S., & Linhardt, R. J. (1989) *Thromb. Res. 53*, 55–71.

Lindahl, U., & Kjellén, L. (1987) in *The Biology of the Extracellular Matrix: Proteoglycans* (Weight, T. N., & Mecham, R., Eds.) p 59, Academic Press, New York.

Lindahl, U., Bäckström, G., & Thunberg, L. (1983) *J. Biol. Chem. 258*, 9826–9830.

Lindahl, U., Thunberg, L, Bäckström, G., Riesenfeld, J., Nordling, K., & Bjork, I. (1984) *J. Biol. Chem. 259*, 12368–12376.

Lindahl, U., Feingold, D. S., & Rodén, L. (1986) *Trends Biochem. Sci.*, 221.

Lindhardt, R. J., Rice, K. G., Merchant, Z. M., Kim, Y. S., & Lohse, D. L. (1986) *J. Biol. Chem. 261*, 14448–14454.

Linhardt, R. J., Rice, K. G., Kim, Y. S., Lohse, D. L., Wang, H. M., & Loganathan, D. (1988) *Biochem. J. 254*, 781–787.

Linker, A., & Hovingh, P. (1984) *Carbohydr. Res. 127*, 75–94.

Mallis, L. M., Wang, H. M., Loganathan, D., & Linhardt, R. J. (1989) *Anal. Chem. 61*, 1453–1458.

Merchant, Z. M., Kim, Y. S., Rice, K. G., & Linhardt, R. J. (1985) *Biochem. J. 229*, 369–377.

Pejler, G., Danielsson, A., Bjork, I., Lindahl, U., Nader, H. B., & Dietrich, C. P. (1987) *J. Biol. Chem. 262*, 11413–11421.

Perlin, A. S., & Folkman, J. (1987) *Thromb. Hemostasis 58*, 792.
Petitou, M., Lormeau, J.-C., Perly, B., Berthault, P., Bossennec, V., Sie, P., & Choay, J. (1988) *J. Biol. Chem. 263*, 8685-8690.
Ragazzi, M., Ferro, D. R., Perly, B., Torri, G., Casu, B., Sinaÿ, P., Petitou, M., & Choay, J. (1987) *Carbohydr. Res. 165*, c1-c5.
Rice, K. G., & Linhardt, R. J. (1989) *Carbohydr. Res. 190*, 219-233.
Rice, K. G., Kim, Y. S., Grant, A. C., Merchant, Z. M., & Linhardt, R. J. (1985) *Anal. Biochem. 150*, 325-331.
Rice, K. G., Rottink, M. K., & Linhardt, R. J. (1987) *Biochem. J. 244*, 515-522.
Yang, V. C., Linhardt, R. J., Bernstein, H., Cooney, C. L., & Langer, R. (1985) *J. Biol. Chem. 260*, 1849-1857.

Effects of Cholesterol on Conformational Disorder in Dipalmitoylphosphatidylcholine Bilayers. A Quantitative IR Study of the Depth Dependence†

M. A. Davies, H. F. Schuster, J. W. Brauner, and R. Mendelsohn*
Department of Chemistry, Newark College of Arts and Science, Rutgers University, 73 Warren Street, Newark, New Jersey 07102

Received November 13, 1989; Revised Manuscript Received January 10, 1990

ABSTRACT: A method originally proposed by Snyder and Poore [(1973) *Macromolecules 6*, 708-715] as a specific probe of trans-gauche isomerization in hydrocarbon chains and recently applied [Mendelsohn et al. (1989) *Biochemistry 28*, 8934-8939] to the quantitative determination of phospholipid acyl chain conformational order is utilized to monitor the effects of cholesterol at various depths in dipalmitoylphosphatidylcholine (DPPC) bilayers. The method is based on the observation that the CD_2 rocking modes from the acyl chains of specifically deuterated phospholipids occur at frequencies in the Fourier transform infrared spectrum which depend upon the local geometry (trans or gauche) of the C-C-C skeleton surrounding a central CD_2 group. Three specifically deuterated derivatives of DPPC, namely, 4,4,4′,4′-d_4 DPPC (4-d_4 DPPC), 6,6,6′,6′-d_4 DPPC (6-d_4 DPPC), and 12,12,12′,12′-d_4 DPPC (12-d_4 DPPC), have been synthesized, and the effects of cholesterol addition at 2:1 DPPC/cholesterol (mol:mol) on acyl chain order at various temperatures have been determined. At 48 °C, cholesterol inhibits gauche rotamer formation by factors of ~9 and ~6 at positions 6 and 4, respectively, of the acyl chains, thus demonstrating a strong ordering effect in regions of the bilayer where the sterol rings are presumed to insert parallel to the DPPC acyl chains. In contrast, the ability of the sterol to order the acyl chains is much reduced at the 12-position. The sterol demonstrates only a slight disordering of phospholipid gel phases. Finally, the contributions of different classes of gauche conformers to the spectra have been determined. Kinks and single gauche bends dominate the disordering process as the temperature is increased, although acyl chains with multiple gauche forms are noted at low temperatures. These data are discussed in terms of current models for the effect of cholesterol on phospholipid order and phase properties.

Despite two decades of biophysical studies aimed toward an understanding of cholesterol/phospholid (PL)[1] interaction [for a recent review, see Presti (1985)], a complete description of how PL motion and order are altered by the sterol has not yet been achieved. A plethora of spectroscopic methods such as electron spin resonance (ESR) (Hubbell & McConnell, 1971; Boggs & Hsia, 1972; Marsh & Smith, 1973; Delmelle et al., 1980), Raman (Lippert & Peticolas, 1971; Mendelsohn, 1972), Fourier transform infrared (FT-IR) (Umemura et al., 1980), and ^2H NMR (Stockton et al., 1976) spectroscopies have led to the generally accepted conception that cholesterol fluidizes and/or disorders phospholipids below their gel-liquid-crystal phase transition temperature (T_m) while rigidifying phospholipids at temperatures above T_m. A simple, specific structural model (Rothman & Engelman, 1972; Hubbell & McConnell, 1971) has been proposed in which PL acyl chain conformational disorder is restricted by the sterol ring structure for a distance of about 11 Å into the bilayer from the interfacial region. In contrast, those acyl chain segments that protrude beyond this bulky region of sterol (i.e., toward the bilayer center) are thought to possess enhanced conformational flexibility due to poor packaging between themselves and the chain region of the sterol.

In addition to the above microscopic description of cholesterol-induced alterations in PL structure and order, the phase properties of PL/cholesterol mixtures have been widely probed. High-sensitivity differential scanning calorimetry (DSC) (Mabrey et al., 1978) has demonstrated the coexistence of two domains in mixtures of saturated phosphatidylcholines (PCs) and cholesterol. One corresponds to a relatively pure PC phase, the second to a binary cholesterol/PC complex. The

† Supported by grants to R.M. from PHS (GM-29864) and from the Busch bequest to Rutgers University.
* Address correspondence to this author.

[1] Abbreviations: DPPC, dipalmitoylphosphatidylcholine; 4,4,4′,4′-d_4 DPPC, 4-d_4 DPPC; 6,6,6′,6′-d_4 DPPC, 6-d_4 DPPC; 10,10,10′,10′-d_4 DPPC, 10-d_4 DPPC; 12,12,12′,12′-d_4 DPPC, 12-d_4 DPPC; FT-IR, Fourier transform infrared; ESR, electron spin resonance; T_m, gel-liquid-crystal phase transition temperature; PL, phospholipid; DSC, differential scanning calorimetry; NMR, nuclear magnetic resonance.

0006-2960/90/0429-4368$02.50/0